



Published in final edited form as:

Bioorg Med Chem Lett. 2012 January 1; 22(1): 537–542. doi:10.1016/j.bmcl.2011.10.096.

Discovery, Design and Synthesis of Novel Potent and Selective Sphingosine-1-Phosphate 4 Receptor (S1P₄-R) Agonists

Miguel Guerrero^a, Mariangela Urbano^a, Jian Zhao^a, Melissa Crisp^b, Peter Chase^b, Peter Hodder^{b,c}, Marie-Therese Schaeffer^{d,f}, Steven Brown^{d,f}, Hugh Rosen^{d,e,f}, and Edward Roberts^{a,d,*}

^aDepartment of Chemistry, The Scripps Research Institute, 10550 N. Torrey Pines Rd, La Jolla, CA 92037, United States

^bScripps Research Institute Molecular Screening Center, Lead Identification Division, Translational Research Institute, 130 Scripps Way, Jupiter, FL 33458, United States

^cDepartment of Molecular Therapeutics, Scripps Florida, 130 Scripps Way, Jupiter, FL 33458, United States

^dDepartment of Chemical Physiology, The Scripps Research Institute, 10550 N. Torrey Pines Rd, La Jolla, CA 92037, United States

^eDepartment of Immunology, The Scripps Research Institute, 10550 N. Torrey Pines Rd, La Jolla, CA 92037, United States

^fThe Scripps Research Institute Molecular Screening Center, 10550 N. Torrey Pines Rd, La Jolla, CA 92037, United States

Abstract

High affinity and selective small molecule agonists of the S1P₄ receptor (S1P₄-R) may have significant therapeutic utility in diverse disease areas including autoimmune diseases, viral infections and thrombocytopenia. A high-throughput screening (HTS) of the Molecular Libraries-Small Molecule Repository library identified 3-(2-(2,4-dichlorophenoxy)ethoxy)-6-methyl-2-nitropyridine as a moderately potent and selective S1P₄-R hit agonist. Design, synthesis and systematic structure-activity relationships study of the HTS-derived hit led to the development of novel potent S1P₄-R agonists exquisitely selective over the remaining S1P_{1-3,5}-Rs family members. Remarkably, the molecules herein reported provide novel pharmacological tools to decipher the biological function and assess the therapeutic utility of the S1P₄-R.

Keywords

S1P₄ receptor; selective small molecule S1P₄-R agonists; autoimmune diseases; viral infections; thrombocytopenia

Sphingosine-1-phosphate (S1P) is a sphingolipid mediator formed by the phosphorylation of sphingosine (SPH) and involved in multiple physiological and pathological processes.

© 2011 Elsevier Ltd. All rights reserved.

*Corresponding author. eroberts@scripps.edu, Phone: +1 858-784-7770, FAX: +1 858-784-7745.

Publisher's Disclaimer: This is a PDF file of an unedited manuscript that has been accepted for publication. As a service to our customers we are providing this early version of the manuscript. The manuscript will undergo copyediting, typesetting, and review of the resulting proof before it is published in its final citable form. Please note that during the production process errors may be discovered which could affect the content, and all legal disclaimers that apply to the journal pertain.

Among them, lymphocyte trafficking, angiogenesis, tumorigenesis as well as vascular development and permeability have been extensively explored.¹⁻⁴ The involvement of S1P in these processes results from its ability to modulate important cellular events such as cytoskeletal changes, chemotaxis, survival and proliferation.⁵⁻⁷ It has become clear that the role of S1P in immunological response is not restricted to the regulation of lymphocyte trafficking but extends to the control of immune cell function.⁸ The generation of S1P is mediated by two cytosolic sphingosine kinase isoforms (SPK1 and SPK2) and occurs preferentially in the plasma membrane.^{6,8} The site of action of S1P is not merely intracellular since it is exported out of the cell and binds to five G-protein-coupled receptors named S1P₁₋₅-Rs, in a paracrine or autocrine manner.^{4,6} In addition to its effects on S1P₁₋₅-Rs, S1P can also affect cell function by either binding or modifying putative intracellular targets or by affecting the relative levels of other lipid products, particularly SPH and ceramide whose biological effects oppose those of S1P.^{6,7} S1P_{1,2,3}-Rs are ubiquitously expressed in almost all organs in mice and humans whereas S1P₄-R and S1P₅-R expression is restricted to specific organs and cell types. S1P₄-R is predominately expressed in lymphoid and hematopoietic cells.⁹ S1P₄-R couples to G α_i , G α_o and G $\alpha_{12/13}$ proteins leading to the stimulation of MAPK/ERK signaling pathways, as well as PLC and Rho-Cdc42 activation.^{10,11}

Both, S1P₁-R and S1P₄-R are the most widely expressed S1P-Rs on lymphocytes and dendritic cells (DCs).^{12,13} In contrast to S1P₁-R, the function of S1P₄-R in fundamental immunological processes has been poorly characterized. However, the contribution of S1P₄-R to the immune response is becoming increasingly evident. S1P induces migratory response of murine T-cell lines expressing both S1P₁-R and S1P₄-R mRNA. In D10.G4.1 and EL-4.IL-2 murine cells S1P-induced migration was significantly inhibited by treatment with (S)-FTY720-phosphate, a potent agonist at S1P₁-R and S1P₄-R. In murine CHO cells co-expressing S1P₄-R and S1P₁-R on the cell surface S1P-induced T-cell migration involved the activation of Rho family small GTPase, Cdc42 and Rac. These results have suggested that the association of S1P₄-R and S1P₁-R may play an important role in the migratory and recirculation response of T-cells toward S1P.¹⁴ Intratracheal delivery of synthetic sphingosine analogs with mixed activity over S1P_{1,3-5}-Rs efficiently inhibited the T-cell response to influenza virus infection by impeding the accumulation of DCs in draining lymph nodes. The inhibitory effects were not observed upon specific chemical activation of S1P₁-R, and persisted in S1P₃-R null mice. Based on these findings and on the observation that S1P₅-R expression in DCs is very low whereas S1P₄-R is highly expressed, it has been hypothesized that the S1P₄-R modulation in the lung may be effective at controlling the immunopathological response to viral infections.^{15,16}

S1P₄-R signaling has been proposed to negatively affect T-cell proliferation and modify the cytokine secretion profile of T-lymphocytes.¹⁷ However, these observations were derived from S1P₄-R overexpressing cell lines and need further confirmation. Recently, S1P₄-R has been implicated in the regulation of DC function and T_H17 T-cell differentiation in a murine model.¹⁸ Interestingly, S1P₄-R-mediated S1P signaling also modifies the course of various immune diseases in a murine model. Hence, it has been hypothesized that S1P₄-R may constitute an interesting target to influence the course of various autoimmune diseases.

In vitro and *in vivo* experiments have indicated an additional potential therapeutic application of S1P₄-R molecule modulators in the terminal differentiation of megakaryocytes. Namely, the application of S1P₄-R antagonists might be exploited for inhibiting potentially detrimental reactive thrombocytosis, whereas S1P₄-R agonists represent a potential therapeutic approach for stimulating platelet repopulation after thrombocytopenia.¹⁹

To date, despite the S1P₄-R therapeutic potential, the *in vivo* function of the target receptor remains largely unknown due to the paucity of selective small molecules S1P₄-R modulators.

Recently, our research group identified the 3-methyl-2-((2-methoxyethyl)imino)thiazolidin-4-one **1** as a novel and selective S1P₄-R agonist (Figure 1).²⁰ Herein we report on the discovery and structure-activity relationships (SAR) of novel potent and selective S1P₄-R agonists based on the hit 3-(2-(2,4-dichlorophenoxy)ethoxy)-6-methyl-2-nitropyridine **2**. A high-throughput screening (HTS) of the Molecular Libraries-Small Molecule Repository (MLSMR) library identified **2** as a novel, moderately potent and selective S1P₄-R agonist. The structural integrity of the hit was corroborated by the resynthesis (Scheme 1) of the title compound that showed confirmed EC₅₀'s of 162 nM at S1P₄-R and no agonistic activity at S1P_{1-3,5}-Rs at concentrations up to 25 μM (Figure 1).

Our SAR studies commenced varying the 2,4-dichlorophenyl coil of the hit as outlined in Scheme 1. Alkylation of 3-hydroxypyridine **3** with 1,2-dibromoethane **4** led to the key intermediate **5**, which was subsequently reacted with various hydroxyaryl derivatives **7** to furnish compounds **8a–8s**. The biological results of the entitle molecules are listed in Table 1.²³

Removal of the chlorine from positions 2 and/or 4 of the aromatic ring (**8a**, **8b**, **8f**) led to complete loss of activity. Dichloro-regioisomers **8c**, **8d**, **8e** and 2-chloro-4-phenyl analog **8l** were also inactive. Drastic loss of potency was observed when the chlorines were substituted with fluorine at one or both positions (**8m**, **8n**, **8o**) as well as for the 2- or 4-methoxy derivatives (**8j**, **8i**) and for the 2,4-dimethyl analog (**8k**). Interestingly, the 4-nitro derivative **8p** showed weak but similar activity compared to the 4-chloro analog **8m**. The pyridinyl derivative **8q** resulted in a 22-fold decrease in potency compared to the hit. Conversely, the potency remained similar by replacing the chlorine at position 2 or 4 with bromine (**8g**, **8h**). Interestingly, the 4-bromo-2-trifluoromethyl analog **8r** was only 3-fold less potent than the corresponding 2-chloro analog **8h**. The symmetrically substituted 2,4,6-trichloro-phenyl analog **8s** was also 3-fold less potent than the hit suggesting a steric clash of the trisubstituted phenyl ring within the binding pocket.

Next, we synthesized compounds **13a–13g** (Schemes 2–6) in order to explore the ethylenedioxy spacer while maintaining the 2,4-dichlorophenyl coil and the 6-methyl-2-nitropyridine polar head.

Intermediate **9** was synthesized by alkylating 2,4-dichlorophenol **6** with 1,3-dibromopropane under basic conditions. Alcohol **10** was reacted with phosphorus tribromide (PBr₃) at room temperature to furnish the corresponding bromide **11**. Compounds **13a**, **13b** and **13c** were obtained by the alkylation of **3** with **9**, **11** and **12** respectively under basic conditions (Scheme 2).

Commercially available carboxylic acid **14** was converted into the corresponding acyl chloride using thionyl chloride (SOCl₂) followed by condensation with **3** to furnish the desired product **13d** (Scheme 3).

The cyclopentene oxide **15** was reacted with **6** followed by mesylation of the alcohol intermediate to furnish the mesylated derivative **16**. The final cyclic compound **13e** was obtained by condensation of **3** with **16** (Scheme 4).

The aza-analog **13f** was obtained via aromatic nucleophilic substitution of commercially available triflate **17** with amine **18** (Scheme 5).

The oxazolo[4,5-*b*]pyridine **13g** was synthesized by condensing hydroxypyridine **19** with carboxylic acid **14** using polyphosphoric acid (PPA) (Scheme 6).

The biological results of **13a–13f** are listed in Table 2.

Elongating the alkyl chain (**13a**) as well as introducing a carbonyl group (**13d**) resulted in complete loss of activity. Furthermore, the constrained 5-membered ring analog **13e** was inactive. Interestingly, the methylene analogs **13c** and **13b** were respectively inactive and 5–6 fold less active than the hit suggesting that the replaced oxygen might be involved in a hydrogen bond interaction. Surprisingly, the aza-analog **13f** was inactive suggesting that the hydrogen bond acceptor capability in this portion of the molecule is an essential binding requirement. Merging the spacer and the head led to oxazolo[4,5-*b*]pyridine **13g**, which was found inactive in concentrations up to 25 μM . Cumulatively, these data suggest that the ethylenedioxy spacer is an essential structural feature for the binding activity and is highly restricted in terms of length, bulkiness and conformation.

Successively, we focused on the study of the polar head while retaining the 2,4-dichlorophenyl coil and the ethylenedioxy chain. The synthesis of the target molecules **22a–22aa** is represented in Scheme 7. The alkylation of **6** with **4** yielded the key bromide intermediate **20**. A diverse set of hydroxyaryl analogs **21I–21XVIII** was reacted with **20** to furnish the desired products **22a–22e**, **22h–22s**, **22v**. Hydrolysis of methylester **22e** under standard conditions yielded the carboxylic acid **22g**, which was converted into **22f** via standard amide coupling conditions. Methyl pyridine analog **22p** was reacted with *meta*-chloroperbenzoic acid (mCPBA) to form the corresponding N-oxide which was converted into the alcohol derivative **22t** using the Boekelheiden reaction.²¹ Oxidation of **22t** using manganese dioxide (MnO_2) under standard conditions gave aldehyde **22u**. Oxidation of alcohol **22v** using previously described conditions furnished the aldehyde **22w**. Analogs **22y** and **22z** were then synthesized employing the Wittig reaction between aldehyde **22w** and the corresponding phosphonium ylide. The 6-methoxymethyl analog **22x** was synthesized by methylation of the alcohol **22v** with methyl iodide. The fluoro derivative **22aa** was obtained from alcohol **22v** via displacement of the mesylate using tetrabutylammonium fluoride (TBAF).

The biological results of **22a–22aa** are listed in Table 3.

Deletion of the 6-methyl from the hit led to 18-fold loss of activity (**22a**), while removal of the 2-nitro led to the inactive compound **22b**. Interestingly, the phenyl analog **22c** showed a 8-fold loss in potency and a reduced efficacy of 40% suggesting that the basic pyridinyl nitrogen may be involved in a hydrogen bond interaction. Replacing the 6-methyl with chlorine (**22d**) led to only 2-fold decrement in potency. Aware that most nitro-containing compounds can cause methaemoglobinemia and are potentially mutagenic, our synthetic efforts focused on the replacement of the nitro group by a different molecular feature.²² However, the installation of classical nitro-bioisosteres such as methyl ester (**22e**), amide (**22f**) and carboxylic acid (**22g**) led to a great or complete loss of activity. Next, analogs containing hydrogen-bond donor groups were synthesized. Unfortunately, hydroxymethyl (**22h**) and amino (**22i**) analogs were found inactive. These data suggest that the nitro group may not be involved in a hydrogen bond interaction but rather may be directing the ether spacer into the active conformation. In order to investigate this hypothesis, the methyl (**22j**), ethyl (**22k**) and phenyl (**22q**) analogs were synthesized. These analogs were found less active than the hit showing a decrement in potency correlated with the size of the substituent. Finally, we explored the possibility of installing halogen atoms to substitute the nitro group. Remarkably, the 2-bromo **22l** (CYM50199) and the 2,6-dibromo **22n** (CYM50179) analogs were found to be 3-fold more potent than the hit. Restricting the

rotation of the spacer by attaching a methyl group at position 4 of **22l** led to the inactive compound **22s**. Removal of the bromine from position 6 (**22m**) led to significant loss of potency as previously observed with the nitro analog **22a**. The 2-bromo-6-fluoro analog **22o** was only 4-fold less potent than **22l**, but 6-fold more potent than **22m**, suggesting that substituents at position 6 modulate the potency. The 2-iodo-6-methyl analog **22p** (**CYM50138**) was equipotent to the 2-bromo analog **22l**. Based on the acquired information, the SAR at position 6 was further investigated. Substituting the methyl group with a phenyl ring (**22r**) led to a substantial loss of potency. Interestingly, hydroxymethyl **22t** was only 4-fold less potent whereas aldehyde **22u** was 38-fold less active than **22p**, suggesting that a hydrogen-bond donor rather than an acceptor may be better tolerated in this region of the molecule. Interestingly, in the presence of chlorine at position 2 comparable activities were found for both the alcohol **22v** and aldehyde **22w** derivatives, which were respectively 5-fold less and slightly more active than the 2-iodine counterparts (**22t**, **22u**). In line with the hypothesis that a hydrogen-bond acceptor is not well accepted in this region, the methyl ether **22x** was inactive. Successively, we explored the influence of alkenyl substituents in this region. The ethylene analog **22y** showed modest potency, while its dimethylated analog **22z** was inactive suggesting that bulky substituents are detrimental for the potency. Taking into account that halogens directly attached at position 6 of the pyridine ring (**22d**, **22n**, **22o**) were well tolerated probably due to the formation of a dipole, we prepared the fluoromethyl derivative **22aa**. Remarkably, **22aa** (**CYM50260**) was found 3.5-fold more potent than the hit compound and was equipotent to the dibromine analog **22n**. These data suggest that substituents at positions 2 and 6 are essential to improve the potency. The position 2 tolerated nitro and halogen groups while small lipophilic or dipole-inducing groups were the most suitable substituents at position 6.

A set of the most active compounds was selected for selectivity assays against S1P_{1-3,5}-R subtypes (Table 4). Remarkably, all tested compounds displayed exquisite selectivity against the other S1P-R family members.

In summary, we have reported the discovery, design and synthesis of novel small molecule S1P₄-R agonists based on a 3-(2-(phenoxy)ethoxy)-6-alkyl-2-nitropyridine chemotype distinct from previously reported S1P₄-R modulators. Systematic SAR analysis of the original MLSMR hit **2**, a selective but moderately potent S1P₄-R agonist, led to the development of novel potent and exquisitely selective S1P₄-R agonists **22l**, **22n**, **22p**, **22aa** (**CYM50199**, **CYM50179**, **CYM50138**, **CYM50260**). Noteworthy, the studies herein reported provide novel pharmacological tools to decipher the biological function and assess the therapeutic utility of the S1P₄-R. Further studies of our research program will be communicated in due course.

Acknowledgments

This work was supported by the National Institute of Health Molecular Library Probe Production Center grant U54 MH084512 (Edward Roberts, Hugh Rosen) and AI074564 (Michael Oldstone, Hugh Rosen). We thank Mark Southern for data management with Pub Chem, Pierre Baillargeon and Lina DeLuca (Lead Identification Division, Scripps Florida) for compound management.

References and notes

1. Sanchez T, Hla T. *J Cell Biochem.* 2004; 92:913–922. [PubMed: 15258915]
2. Schwab SR, Cyster JG. *Nature Immunol.* 2007; 8:1295–1301. [PubMed: 18026082]
3. Kono M, Allende ML, Proia RL. *Biochim Biophys Acta.* 2008; 1781:435–441. [PubMed: 18675379]
4. Marsolais D, Rosen H. *Nat Rev Drug Discov.* 2009; 8:297–307. [PubMed: 19300460]
5. Fyrst H, Saba JD. *Nat Chem Biol.* 2010; 6:489–497. [PubMed: 20559316]

6. Spiegel S, Milstien S. *Nat Rev Mol Cell Biol.* 2003; 4:397–407. [PubMed: 12728273]
7. Hannun YA, Obeid LM. *Nat Rev Mol Cell Biol.* 2008; 9:139–150. [PubMed: 18216770]
8. Rivera J, Proia RL, Olivera A. *Nat Rev Immunol.* 2008; 8:753–763. [PubMed: 18787560]
9. Gräler MH, Bernhardt G, Lipp M. *Genomics.* 1998; 53:164–169. [PubMed: 9790765]
10. Toman RE, Spiegel S. *Neurochem Res.* 2002; 27:619. [PubMed: 12374197]
11. Kohno T, Matsuyuki H, Inagaki Y, Igarashi Y. *Genes Cells.* 2003; 8:685. [PubMed: 12875654]
12. Goetzl EJ, Rosen H. *J Clin Invest.* 2004; 114:1531–1537. [PubMed: 15578083]
13. Idzko M, Hammad H, van Nimwegen M, Kool M, Muller T, Soullie T, Willart MA, Hijdra D, Hoogsteden HC, Lambrecht BN. *J Clin Invest.* 2006; 116:2935–2944. [PubMed: 17080194]
14. Matsuyuki H, Maeda Y, Yano K, Sugahara K, Chiba K, Kohno T, Igarashi Y. *Cell Mol Immunol.* 2006; 3:429. [PubMed: 17257496]
15. Maeda Y, Matsuyuki H, Shimano K, Kataoka H, Sugahara K, Kenji Chiba K. *J Immunol.* 2007; 178:3437. [PubMed: 17339438]
16. Marsolais D, Hahm B, Edelmann KH, Walsh KB, Guerrero M, Hatta Y, Kawaoka Y, Roberts E, Oldstone MB, Rosen H. *Mol Pharmacol.* 2008; 74:896. [PubMed: 18577684]
17. Wang W, Graeler MH, Goetzl EJ. *FASEB J.* 2005; 19:1731–1733. [PubMed: 16046470]
18. Schulze T, Golfier S, Tabeling C, Räbel K, Gräler MH, Witzentrath M, Lipp M. *FASEB J.* 2011; 25:1096–1097. [PubMed: 21315927]
19. Golfier S, Kondo S, Schulze T, Takeuchi T, Vassileva G, Achtman AH, Gräler MH, Abbondanzo SJ, Wiekowski M, Kremmer E, Endo Y, Lira SA, Bacon KB, Lipp M. *FASEB J.* 2010; 24:4701. [PubMed: 20686109]
20. Urbano M, Guerrero M, Velaparthi S, Crisp M, Chase P, Hodder P, Schaeffer M, Brown S, Rosen H, Roberts E. *Bioorg Med Chem Lett.* 2011; 22:1016–1017. [PubMed: 21315927]
21. Fontenas C, Bejan E, Ait Haddou H, Balavoine GGA. *Synthetic Communications.* 1995; 25:629–633.
22. Smith GF. *Prog Med Chem.* 2011; 50:1. [PubMed: 21315927]
23. The biological assays were performed using Tango S1P₄-BLA U2OS cells containing the human Endothelial Differentiation Gene 6 (EDG6; S1P₄-R) linked to a GAL4-VP16 transcription factor via a TEV protease site. The cells also express a beta-arrestin/TEV protease fusion protein and a beta-lactamase (BLA) reporter gene under the control of a UAS response element. Stimulation of the S1P₄-R by agonist causes migration of the fusion protein to the GPCR, and through proteolysis liberates GAL4-VP16 from the receptor. The liberated VP16-GAL4 migrates to the nucleus, where it induces transcription of the BLA gene. BLA expression is monitored by measuring fluorescence resonance energy transfer (FRET) of a cleavable, fluorogenic, cell-permeable BLA substrate. As designed, test compounds that act as S1P₄-R agonists will activate S1P₄-R and increase well FRET. Compounds were tested in triplicate at a final nominal concentration of 25 micromolar

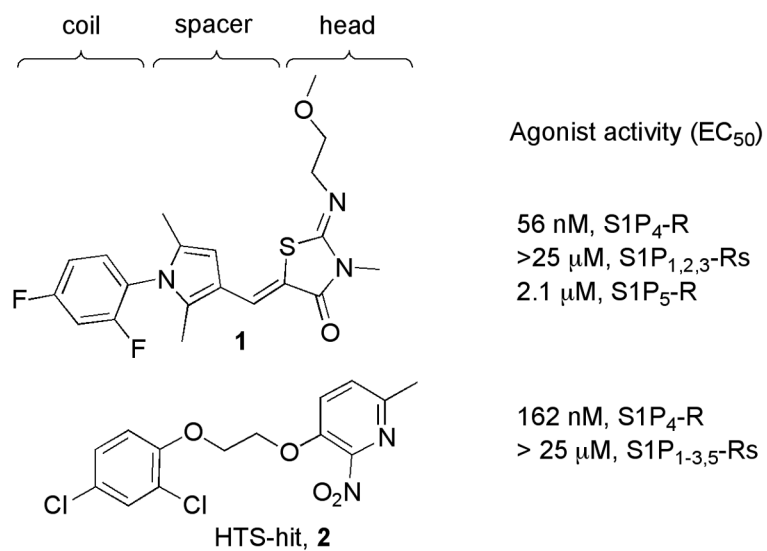
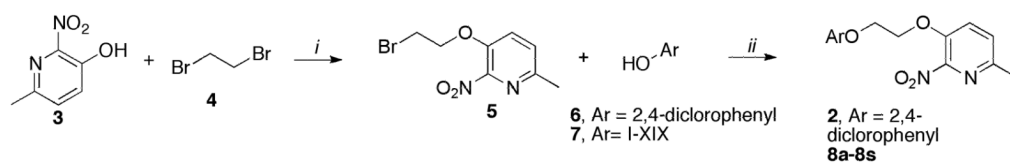
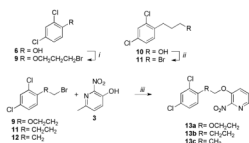


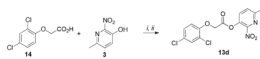
Figure 1.
 Novel and selective S1P₄-R agonists

**Scheme 1.**Synthesis of **8a-8s**

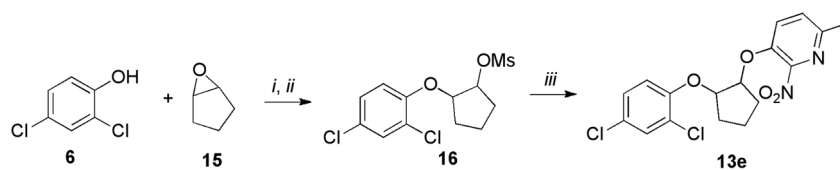
Reagents and conditions (i) **3** (1 equiv.), **4** (4 equiv.), K_2CO_3 (2 equiv.), DMSO, 40°C , 4h, 65%; (ii) **5** (1 equiv.), **6** or **7** (2 equiv.), K_2CO_3 (2 equiv.), DMSO, 40°C , 4h, 50–98%.

**Scheme 2.****Synthesis of 13a, 13b, 13c**

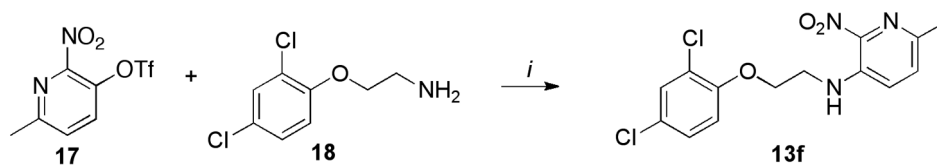
Reagents and conditions: (i) **6** (1 equiv.), 1,3-dibromopropane (4 equiv.), K₂CO₃ (2 equiv.), DMSO, 40°C, 4h, 65%; (ii) **10** (1 equiv.), PBr₃ (0.33 equiv.), CH₂Cl₂, 0°C to rt, 3h, 85%; (iii) **9** or **11** or **12** (1 equiv.), **3** (1 equiv.), K₂CO₃ (2 equiv.), 40°C, 4h, 75–90%.

**Scheme 3.****Synthesis of 13d**

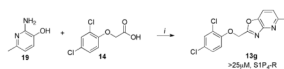
Reagents and conditions: (i) **14** (1 equiv.), SOCl₂, reflux, 2h; (ii) **3** (1.2 equiv.), DIPEA (1.2 equiv.), CH₂Cl₂, 0°C to rt, overnight, 80% (over two steps).

**Scheme 4.****Synthesis of 13e**

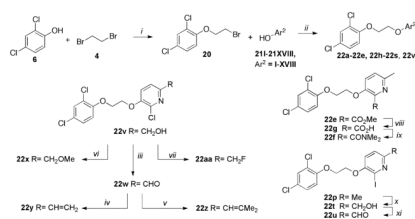
Reagents and conditions: (i) **6** (1 equiv.), **15** (2.1 equiv.), K_2CO_3 (4 equiv.), EtOH, 80°C, overnight; (ii) $MeSO_2Cl$ (2 equiv.), pyridine, 0°C, 6h, 70% (over 2 steps); (iii) (a) **3** (1 equiv.), KOH, $H_2O/EtOH$, 80°C, 30 min; (b) **16** (1 equiv.), DMF, 120°C, overnight, 60%.

**Scheme 5.****Synthesis of 13f**

Reagents and conditions: (i) **17** (1 equiv.), **18** (1 equiv.), DMF, 100°C, 12h, 65%.

**Scheme 6.**Synthesis of **13g**

Reagents and conditions: (i) **19** (1 equiv.), **14** (1.5 equiv.), PPA, 130°C, 2h, 45%.

**Scheme 7.****Synthesis of 22a–22aa**

Reagents and conditions: (i) **6** (1 equiv.), **4** (4 equiv.), K_2CO_3 (2 equiv.), DMSO, 40°C, 6h, 75%; (ii) **20** (1 equiv.), **21I–21XVIII** (1.1 equiv.), K_2CO_3 (1.5 equiv.), DMSO, 40°C, 6h, 70–95%; (iii) **22v** (1 equiv.), MnO_2 (5 equiv.), $CHCl_3$, rt, 3h, 67%; (iv) (a) $CH_3PPh_3^+Br^-$ (2 equiv.), BuLi (2 equiv.), THF, 0°C, 30min; (b) **22w** (1 equiv.), 0°C to rt, 2h, 60%; (v) (a) $(CH_3)_2CHPPh_3^+Br^-$ (2 equiv.), BuLi (2 equiv.), THF, 0°C, 30 min; (b) **22w** (1 equiv.), 0°C to rt, 2h, 40%; (vi) **22v** (1 equiv.), NaH (1.5 equiv.), MeI (5 equiv.), DMF, 0°C to rt, overnight, 72%; (vii) (a) **22v** (1 equiv.), MsCl (1.1 equiv.), Et_3N (3 equiv.), 0°C to rt, overnight; (b) TBAF (1M THF) (1.5 equiv.), acetonitrile, 50°C, 12h, 60% (over two steps); (viii) **22e** (1 equiv.), LiOH (1.1 equiv.), MeOH/THF/ H_2O (3:1:1), rt, 2h, 70%; (ix) **22g** (1 equiv.), $NHMe_2$, HCl (1.2 equiv.), DIPEA (1.2 equiv.), EDCI (1.3 equiv.), HOBt (1.3 equiv.), CH_2Cl_2 , rt, 3h, 88%; (x) (a) **22p** (1 equiv.), MCPBA (12 equiv.), CH_2Cl_2 , rt, 6h; (b) $(CF_3CO)_2O$ (1 equiv.), DMF, 0°C to rt, 24h; (c) Na_2CO_3 , rt, 1h, 39% (over three steps); (xi) **22t** (1 equiv.), MnO_2 (5 equiv.), $CHCl_3$, rt, 3h, 65%.

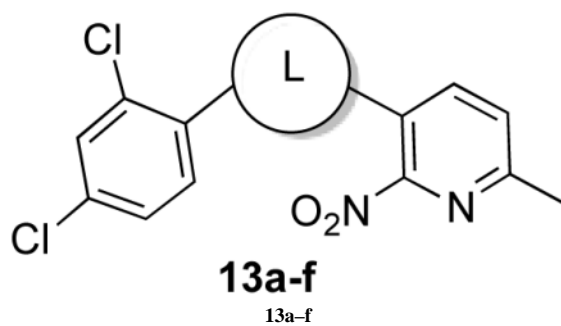
Table 1

S1P₄-R agonist activity of **8a–8s**

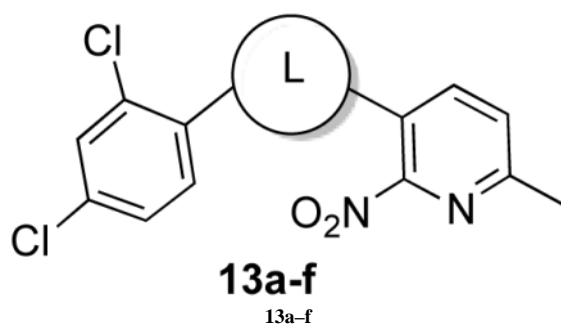
cpd		Ar	EC ₅₀ (nM) ^a
8a	I	2-chlorophenyl	NA
8b	II	4-chlorophenyl	NA
8c	III	2,5-dichlorophenyl	NA
8d	IV	2,3-dichlorophenyl	NA
8e	V	3,4-dichlorophenyl	NA
8f	VI	phenyl	NA
8g	VII	2-bromo-4-chlorophenyl	232
8h	VIII	4-bromo-2-chlorophenyl	220
8i	IX	2-chloro-4-methoxy phenyl	3900
8j	X	4-chloro-2-methoxyphenyl	5400
8k	XI	2,4-dimethylphenyl	7200
8l	XII	2-chloro-4-phenylphenyl	NA
8m	XIII	4-chloro-2-fluorophenyl	3100
8n	XIV	2-chloro-4-fluorophenyl	2600
8o	XV	2,4-difluorophenyl	40% 50μM
8p	XVI	2-fluoro-4-nitrophenyl	2800
8q	XVII	5-chloro-3-nitropyridin-2-yl	3500
8r	XVIII	4-bromo-2-(trifluoromethyl)phenyl	601
8s	XIX	2,4,6-trichlorophenyl	570

^aData are reported as mean of $n = 3$ determinations. NA = not active at concentrations up to 25 μM.

Table 2

S1P₄-R agonist activity of **13a–13f**

cpd	L	EC ₅₀ (nM) ^a
13a		NA
13b		920
13c		NA
13d		NA

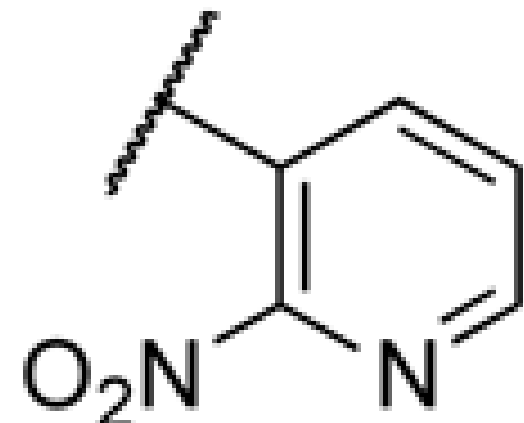
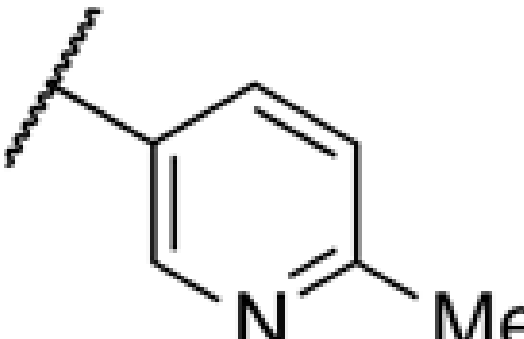
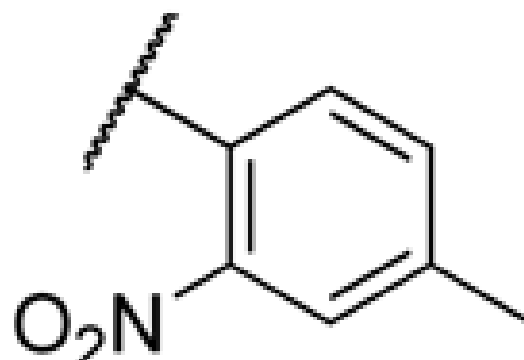
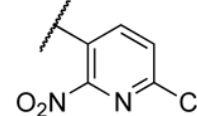


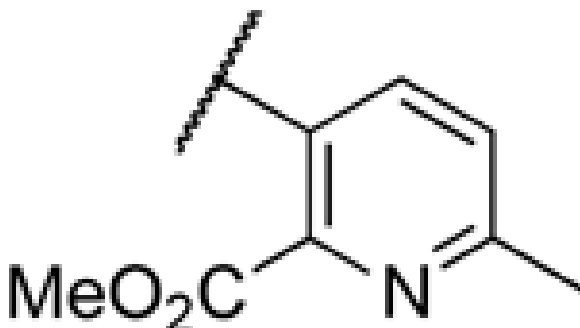
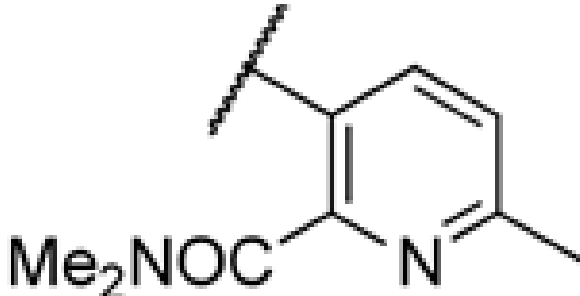
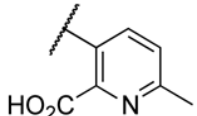
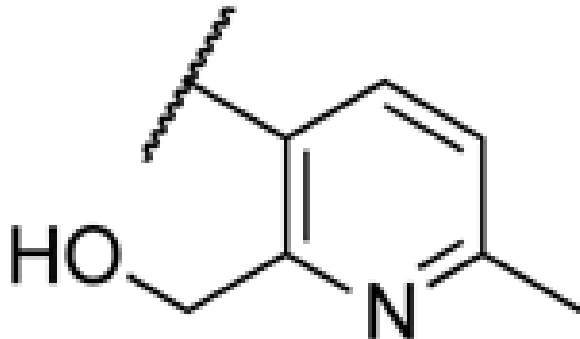
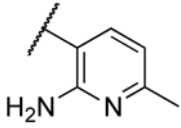
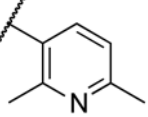
cpd	L	EC ₅₀ (nM) ^a
13e		NA
13f		NA

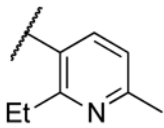
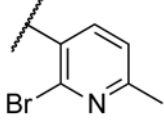
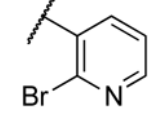
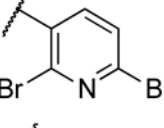
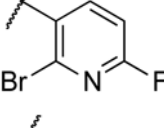
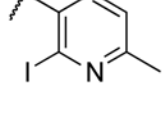
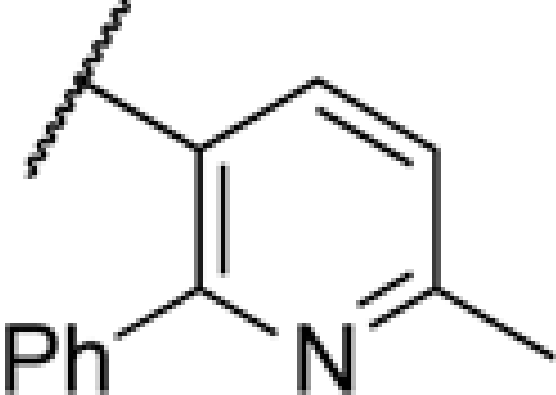
^aData are reported as mean of $n = 3$ determinations. NA = not active at concentrations up to 25 μ M.

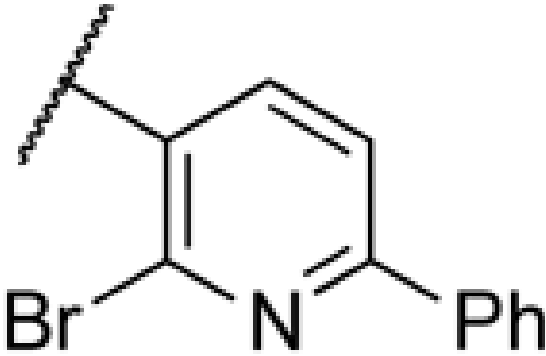
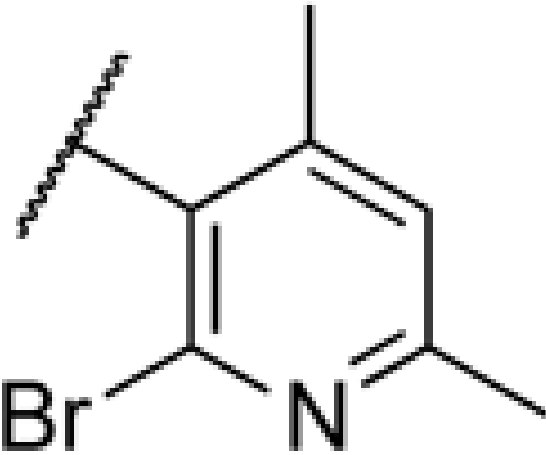
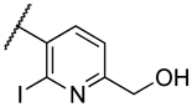
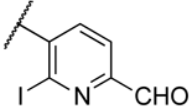
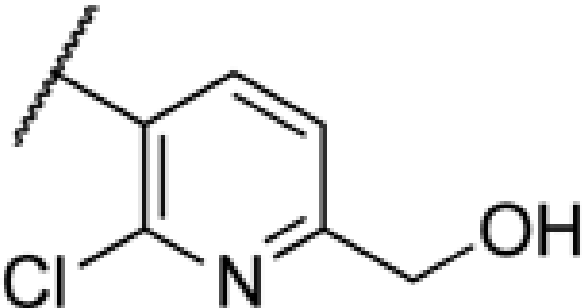
Table 3

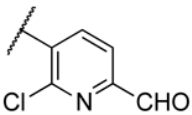
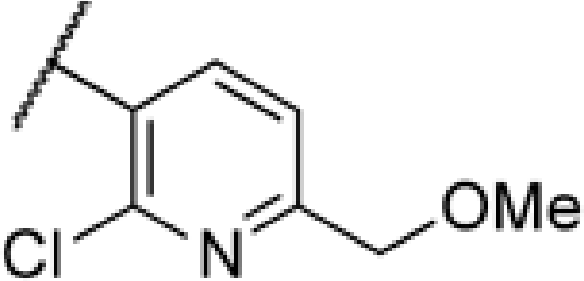
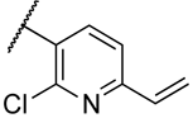
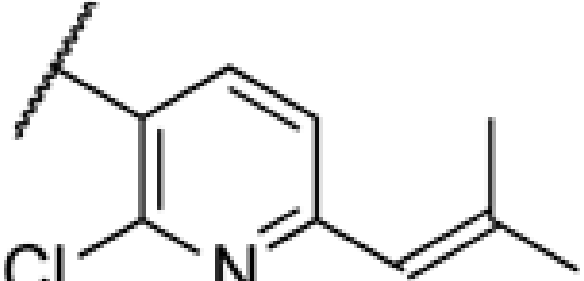
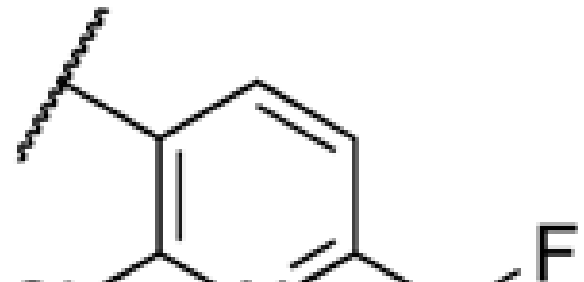
S1P₄-R agonist activity of 22a–22aa

cpd	Ar ²	EC ₅₀ (nM) ^α
22a	I 	2980
22b	II 	NA
22c	III 	1300 (40%) ^β
22d	IV 	304

cpd		Ar ²	EC ₅₀ (nM) ^α
22e	V		4800
22f			NA
22g			NA
22h	VI		NA
22i	VII		NA
22j	VIII		2600 (65%) ^β

cpd		Ar ²	EC ₅₀ (nM) ^a
22k	IX		7300
22l	X		52
22m	XI		1300
22n	XII		46
22o	XIII		208
22p	XIV		54
22q	XV		NA

cpd	Ar ²	EC ₅₀ (nM) ^α
22r XVI		6000 (70%) ^β
22s XVII		NA
22t		287
22u		2100
22v XVIII		1500

cpd	Ar ²	EC ₅₀ (nM) ^a
22w		1800
22x		NA
22y		658
22z		NA
22aa		45

^aData are reported as mean of $n = 3$ determinations.

^bPercentage of response at given concentration. NA = not active at concentrations up to 25 μ M.

Table 4

SIP_{1-3,5}-Rs selectivity counter screen

cpd	EC50 nM ^a				
	SIP ₄ -R	SIP ₁ -R	SIP ₂ -R	SIP ₃ -R	SIP ₅ -R
2	162	NA	NA	NA	NA
8g	232	NA	NA	NA	NA
8h	220	NA	NA	NA	NA
8r	601	NA	NA	NA	NA
8s	570	NA	NA	NA	NA
22d	304	NA	NA	NA	NA
22l	52	NA	NA	NA	NA
22n	46	NA	NA	NA	NA
22p	54	NA	NA	NA	NA
22t	287	NA	NA	NA	NA
22aa	45	NA	NA	NA	NA

^aData are reported as mean of *n* = 3 determinations. NA = not active at concentrations up to 25 μM.